Manifold and Base Casting of Lunenburg Foundry Atlantic Marine Engine

by

Chiaki Kirby

Submitted to the
Department of Mechanical Engineering
in Partial Fulfillment of the Requirements for the Degree of

Bachelor of Science in Mechanical Engineering

at the

Massachusetts Institute of Technology

May 2020

Signature of Author: _____
Department of Mechanical Engineering
May 11, 2020

Certified by: _____
Daniel Braunstein
Senior Lecturer, Pappalardo Design Laboratory Director
Thesis Supervisor

Accepted by: _____
Anette Hosoi
Professor of Mechanical Engineering
Undergraduate Officer

Manifold and Base Casting of Lunenburg Foundry Atlantic Marine Engine

by

Chiaki Kirby

Submitted to the Department of Mechanical Engineering
on May 11, 2020 in Partial Fulfillment of the
Requirements for the Degree of

Bachelor of Science in Mechanical Engineering

Abstract

Previous work started by mechanical engineering students in the spring of 2016 established a basis for applying modern machining and modeling techniques to the fabrication of century old sand cast designs, specifically a Lunenburg Foundry Atlantic Engine. This project was continued by mechanical engineering students in the spring of 2019. From there, this groundwork was used to fabricate one of the remaining parts of the engine, the lower base. Due to COVID-19 pandemic and MIT campus shut down, this thesis project was virtualized. From this, casting simulation software (Visual Cast) used to simulate the casting of another engine part, the manifold, with a variety of geometries and process conditions. The simulations were completed to predict the casting quality of the part if physically cast. Additionally, the next steps for completion of the engine are outlined.

Thesis Supervisor: Daniel Braunstein
Title: Senior Lecturer, Pappalardo Design Laboratory Director

Acknowledgements

I would like to thank Daniel Braunstein, Bill Cormier, James Dudley, Steve Haberek, and Tasker Smith of the Pappalardo Design Laboratory for their support on this project and so much more. The Pappalardo lab has been the foundation of my love for the MIT Mechanical Engineering Department, and I would not be the engineer I am becoming without it. I would also like to thank Mike Tarkanian and James Hunter of the Materials Science Foundry for guidance and participation in casting and the shift to the virtual casting format.

Table of Contents

List of Figures

1. Introduction

As time has passed and technology has progressed, designs and devices that were once widespread and integral parts of day to day life have been redesigned and replaced. The traditional techniques have made way for a new age of manufacturing and fabrication. Modern and traditional techniques and designs have their place and role, and new lessons can be learned from it all at any point. This is made evident by the lessons learned during the recreation of a 1900s marine engine, using modern manufacturing methods in addition to more traditional casting methods. This project adds a degree of modernization to that, using casting simulation software to visualize castings without having to create any, allowing for highly detailed analysis of a casting and a better understanding of any defects that a casting may include. However, this is not to say that developing a flawless simulated casting will without a doubt lead to a flawless physical casting, but lessons learned from applying these modern methods will work alongside lessons learned from fabricating physical castings, allowing for a great breadth of knowledge.

2. The Lunenburg Foundry and the Atlantic Marine Engine

2.1. The History of the Lunenburg Foundry

Officially named Lunenburg Foundry & Engineering Limited, the Lunenburg foundry was established in 1891 in Nova Scotia, Canada. They boast a long history of servicing both marine and domestic industries in the form of a variety of types of equipment, from marine engines to cast iron wood stoves. The focus of this thesis, the Atlantic Engine, was designed and built at the Foundry beginning through the 1920's, with the Foundry being an early pioneer in the development of a marine internal combustion engine. As technology developed, the Foundry developed along with it, eventually advancing beyond the Atlantic engine. The Foundry underwent a significant modernization in the late 1980's, shifting gears and focusing largely on servicing. The Foundry is currently known by the acronym LIFE (Lunenburg Industrial Foundry & Engineering) and provides expertise in ship servicing, fabrication, machining, and metal casting [1]. The Foundry is known for their incredible attention and care for their customers, and the success of the Atlantic engine project is evidence of that supportive nature.

2.2. The Atlantic Marine Engine

"In Lunenburg, the first Atlantic marine engine was created in 1907 by a company that would ultimately outlast every one of its contemporaries in the U.S. and Canada," [2]. The Lunenburg Foundry Atlantic marine engine, an engine first designed over a century ago, is a two-stroke, one-lunger, make and break engine. To elaborate on the style of engine, two-stroke engines run the engine cycle in two strokes, the upward motion and the downward motion of the piston within the cylinder. One-lunger refers to the engine having a single cylinder, a term that originated in New England in the early 1900s due to the distinctive exhaust note the commonly used single cylinder models created. Make and break is the style of ignition system used in the Atlantic, in which the two contact points "make" and then "break", which creates an arc that ignites the fuel-air mixture in the combustion chamber of the cylinder. The Atlantic is a

largely cast iron engine, which is an excellent choice for a marine engine because grey iron is easily cast, cheap, strong, and easily machined. When originally designed, the Atlantic was created using the traditional techniques and methods, such as hand drawn engineering drawings and hand carved soft wood patterns.

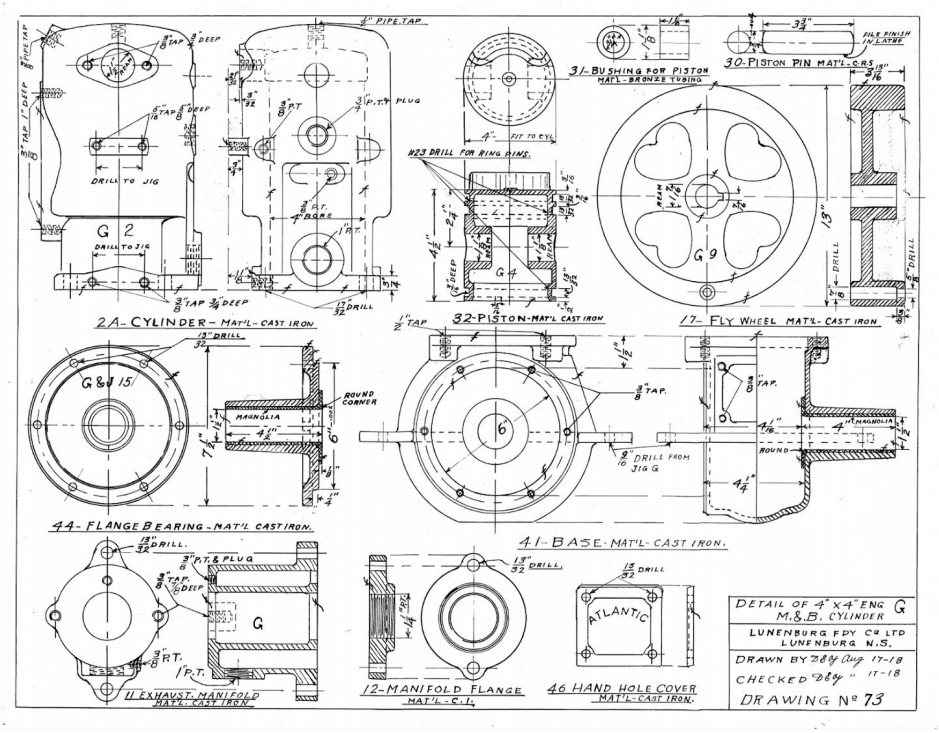

Figure 2-1: An example of the hand drawn engineering drawings created for the Atlantic engine [3].

Figure 2-2: An example of a wood carved pattern, specifically the pattern for the Atlantic cylinder.

While a stunning and highly functional engine, the Atlantic engine decreased in production as more efficient engines, such as four-stroke models, were developed. The last Atlantic engine manufactured by the Lunenburg Foundry was made in the 1990's, and that was by special request as the

Foundry had already stopped manufacturing the Atlantic by that point. This thesis project is a continuation of an effort started by a group of mechanical engineering students in the spring of 2016: to recreate a J model of the Lunenburg Atlantic marine engine using modern modeling and fabrication methods.

3. The Two-Stroke Engine Cycle

Two-stroke engines, as the name indicates, function as a combination of two strokes. Two-stroke engines perform the same function as four-stroke engines, but in half the strokes. The first stroke, intake and compression, occurs as the piston moves up the cylinder. The second stroke, power and exhaust, occurs as the piston moves down the cylinder. As the piston moves up, a vacuum is created in the crankcase, which pulls the fuel-air mixture into the crankcase through the intake port, which is a passive valve. Once the piston reaches its peak, it returns downwards in the second stroke, closing the pressure valve and compressing the fuel mixture in the crankcase. When the piston nears the bottom of its stroke, the transfer port is exposed, allowing the fuel mixture to flow into the main cylinder and push the exhaust out of the now exposed exhaust port. The piston then moves back up into the cylinder, compressing the fuel-air mixture in the combustion chamber. Simultaneously, the lower chamber fills with new fuel-air mixture, which is why the engine is described as two-stroke. As the piston reaches the top of the stroke and the fuel-air mixture is highly compressed, the spark plug ignites the fuel, driving the piston down, creating the power stroke and spinning the flywheel. This once again leads to the exhaust being driven out of the combustion chamber by a new fuel-air mixture, and the process continues as the flywheel pushes the piston back up the cylinder [4].

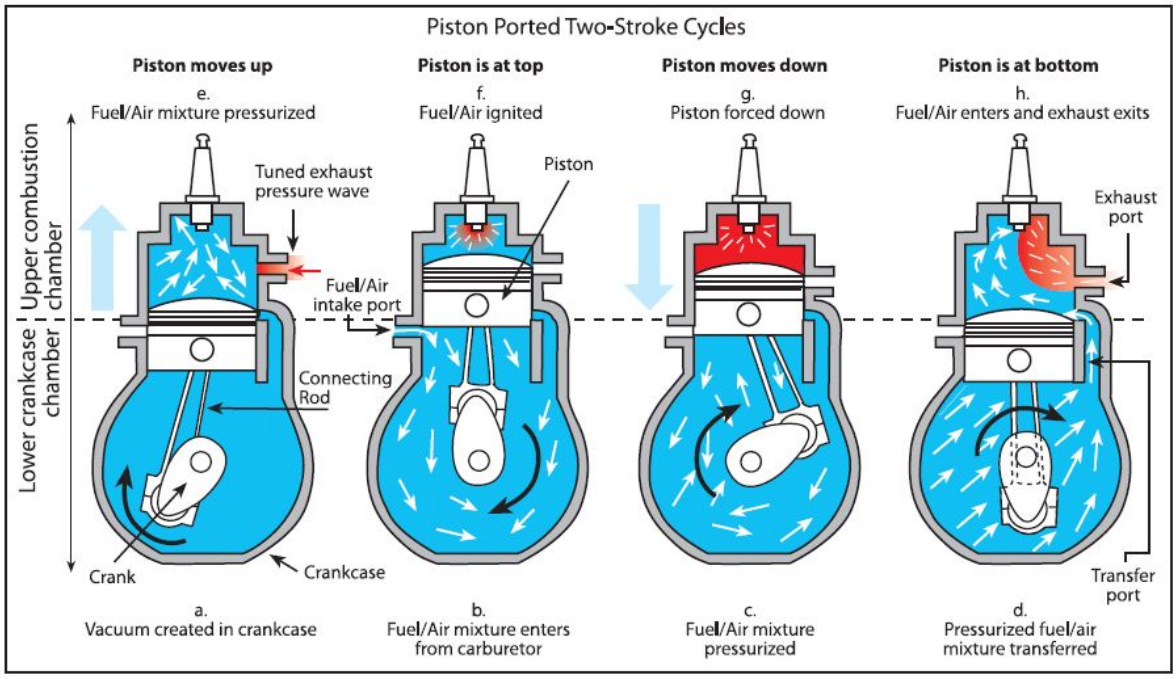

Figure 3-1: Diagram explaining the two-stroke engine cycle, including flow of fuel-air mixture [4].

In comparison to four-stroke engines, two-stroke engines require fewer parts, are lighter, are cheaper, are simpler, and deliver twice as many power strokes per revolution. However, a major drawback is that the passive nature of the ports, especially the exhaust port, results in two-stroke engines being considered "dirty" because unburnt fuel is released from the combustion chamber along with the exhaust, resulting in lower efficiency, dirtier emissions, and increased fuel waste in comparison to four-stroke engines. Fuel efficiency, reduced emissions, and longer lifespan are benefits of four-stroke engines that have led to their wide adoption throughout a variety of industries [5].

4. The Pappalardo Atlantic Engine Project

4.1. Birth of the Project (Spring 2016)

In the spring of 2016, a team of mechanical engineering seniors began a project to recreate a J model of the Lunenburg Foundry Atlantic Marine Engine. The group of students included Gordon Mosely P. Andrews, Josh Born, Samantha Nicole Castellanos, Meaghan Fitzgerald, Kyle Joba-Woodruff, Eric Kline, Brady Knight, Sally Miller, Jarrod Smith, and Emma Steinhardt. The students worked as the first group of senior apprentices in the Pappalardo machine shop, and additionally had the support of Peter Kinley (CEO of Lunenburg Foundry Engineering Limited), the resources and team at the Lunenburg Foundry, and the MIT Materials Science Foundry. As a group, they began work on a majority of the engine parts, managing to create finished versions of a handful of the components by the end of the academic year. Since the spring of 2016 was the first year of the senior Pappalardo apprenticeship project, the bulk of the work the team completed ended up being process testing and verifying. The team developed the CAD models and initial patterns, testing their methods along the way to develop an understanding of the modern techniques that could be used to recreate this roughly century old engine. These students set the groundwork for a complex and extensive project, with the hopes that the engine could be finished by later students.

4.2. Continuation of Work

During the spring of 2019, the senior apprentices in the Pappalardo machine shop continued the work that had been started three years prior. A group of seven mechanical engineering seniors (Tom Frejowski, ZhiYi Liang, Shannon McCoy, Alvaro Meléndez, Coby Nettleton, Matt Quejada, and Sarah Tress) began the semester hoping to complete the work started by the team in 2016, and managed to make great progress. By the end of the academic year there were only four parts remaining: the manifold, the upper base, the lower base, and the cylinder. Attempts had been made on the manifold by Matt Quejada, the lower base by Alvaro Meléndez, and the cylinder by Shannon McCoy. The goal of this thesis project was initially to complete all the remaining parts, assemble, and test the full engine, but the spring 2020 semester was interrupted by the COVID-19 pandemic. Due to the sudden online nature of the project, and the inability to access the Pappalardo machine shop or Materials Science Foundry, modifications were made to this thesis project to develop understanding of casting methods and variables to continue making progress on completing the engine in later semesters.

5. The Lower Base

The lower base of the Atlantic engine serves a few critical roles. When combined with the upper base, it becomes the housing for the crankshaft, providing a bearing surface as the crankshaft drives the connecting rod and the piston through the cylinder. The base is the component of the engine that is mounted to the boat, providing a sturdy structure for the engine. Additionally, as shown in the two-stroke engine cycle, the fuel-air mixture is drawn into the base cavity and is from there directed into the combustion chamber to be pressurized and lit.

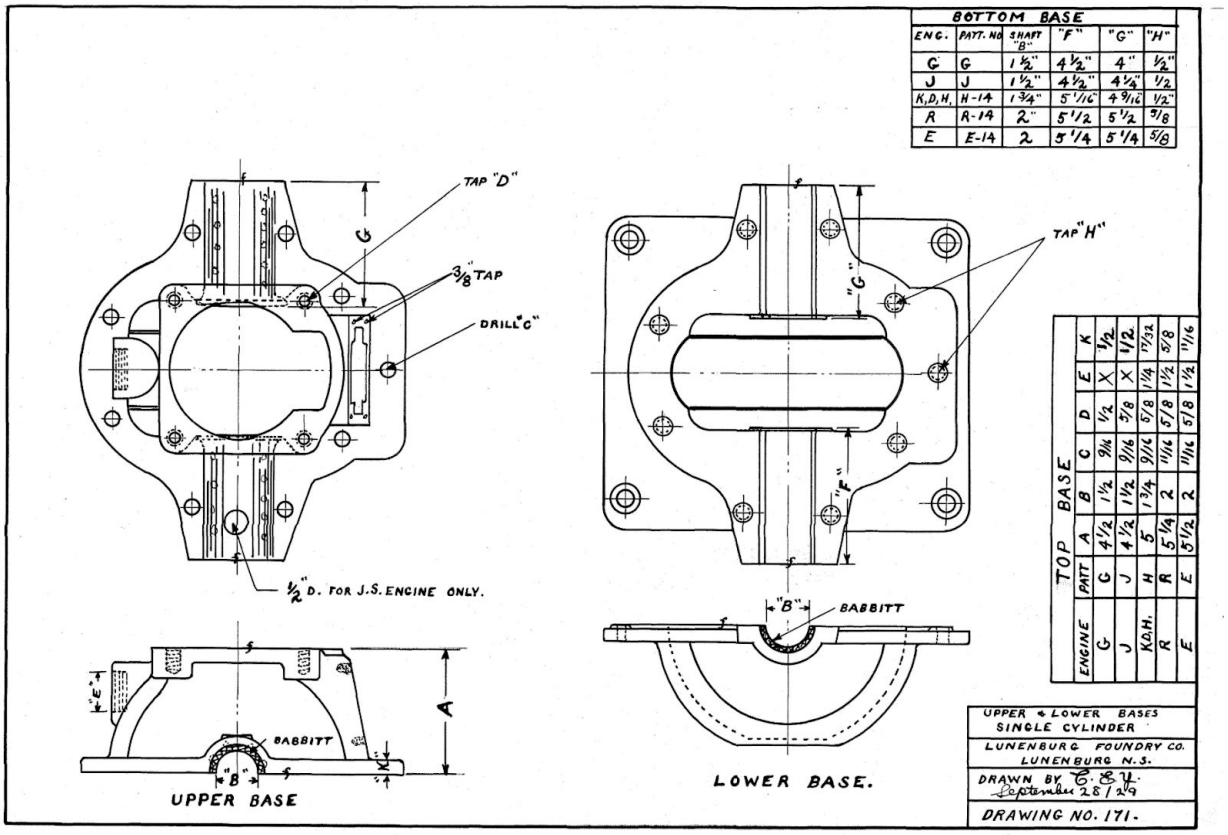

Figure 5-1: Engineering drawings of the upper and lower base parts of the Atlantic J model engine [3].

5.1. Previous Attempts

The first student to work on the base, both lower and upper parts, was Kyle Joba-Woodruff in the spring of 2016. Over the course of the semester, Joba-Woodruff created the initial CAD models of the parts and the first iteration of pattern and core box designs for the sand casting. Due to time constraints, he was unable to attempt to cast the part before the end of the academic year.

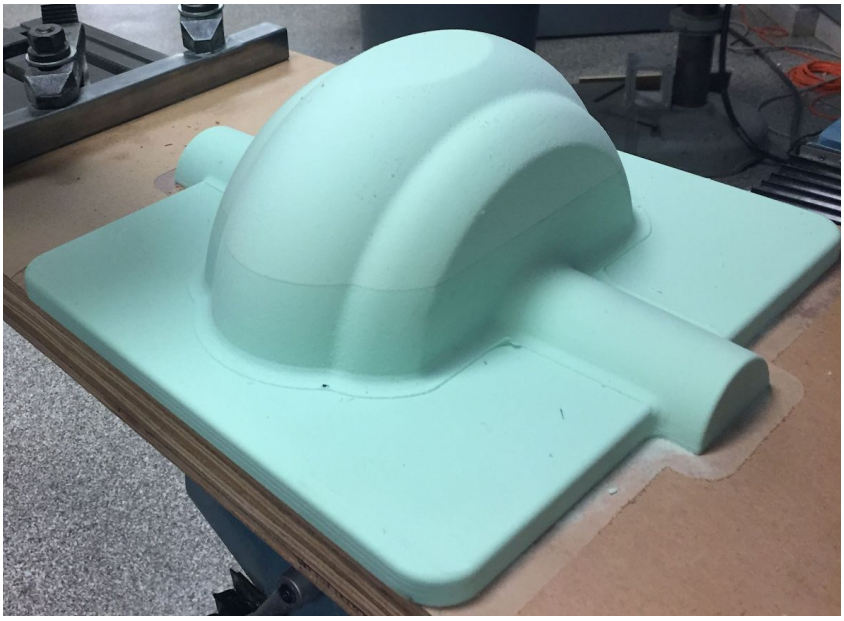

Figure 5-2: Lower base pattern designed and machined by Kyle Joba-Woodruff; Spring 2016.

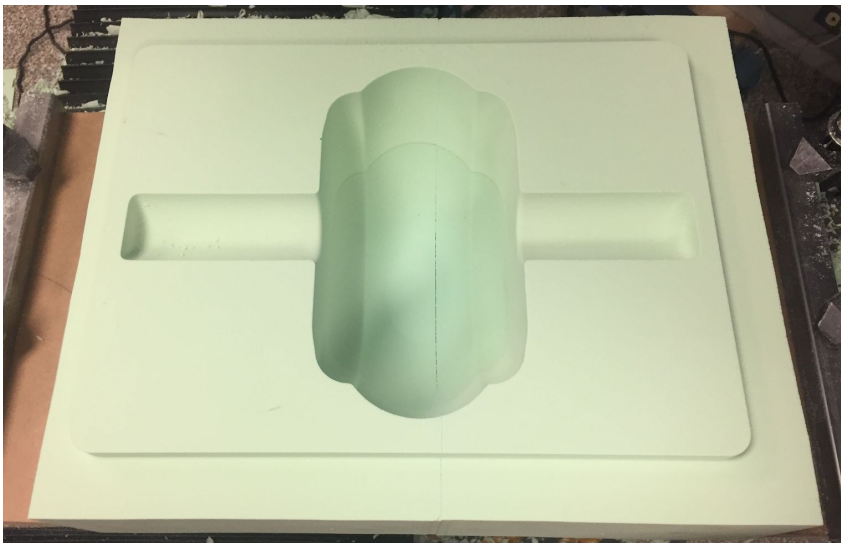

Figure 5-3: Lower base core box designed and machined by Kyle Joba-Woodruff; Spring 2016.

During the spring of 2019, Alvaro Meléndez built off of the existing body of work, and was able to complete the first pour of the lower base. However, Meléndez discovered some issues once the casting was broken out. The pattern and core box were both made perfectly, resulting in a well packed flask and a solid resin bonded core. However, while the part may look symmetrical at a glance, the bearing surfaces for the crankshaft are slightly different lengths, resulting in minor differences in the pattern and the core print. As a result, the core is almost symmetrical, but extends further on one end than the other. When assembling the flask for pouring, the core was placed into the flask in the wrong orientation, causing the main body of the core to be off-center. This led to the wall thickness being inconsistent, and a concern for the lower base breaking and the connecting rod and crankshaft crashing into the walls. The key lesson

learned from this is that it is critical to make sure the orientation and location of all components is correct, which can be done by using different labeling or marking techniques to make sure it is clear which orientation is correct.

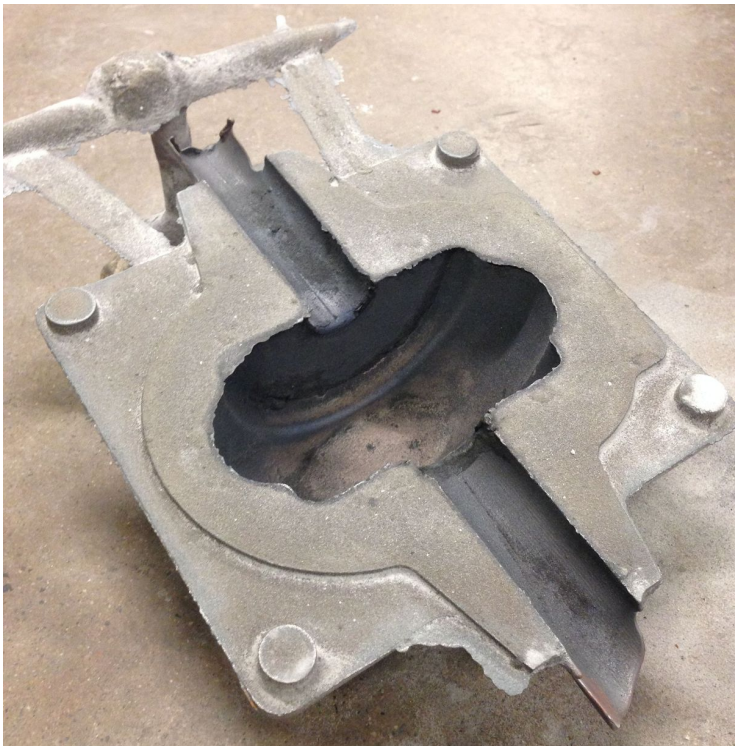

Figure 5-4: First casting of the lower base, fabricated by Alvaro Meléndez; Spring 2019.

Figure 5-5: Close-up image of the first casting of the lower base, fabricated by Alvaro Meléndez; Spring 2019.

5.2. Casting the Lower Base

Building off of the work completed by Joba-Woodruff and Meléndez, this project began with casting the lower base in September of 2019, shortly after the academic year began. The pattern and core box made by the previous students were perfect, so this part was a simple introduction into the basics of sand casting, without the complexities of modifying CAD or creating CNC milled patterns.

The core was created using resin bonded sand packed into the three separate components of the core boxes, and once each component had cured they were glued together to create the entire core. Using a simple wooden flask, the lower base pattern was coated in talcum powder to prevent the green sand from sticking to the pattern, then sand was packed into the flask. The drag and cope were created using this method. The core was then placed inside the flask before pouring.

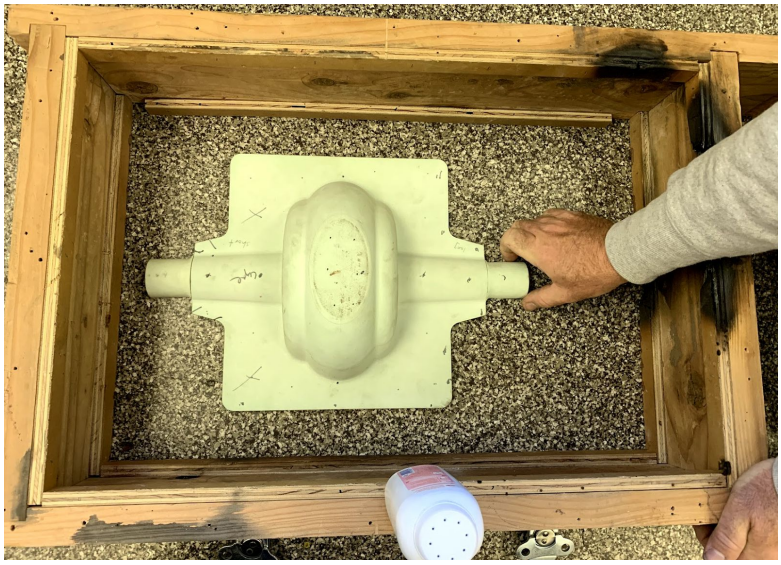

Figure 5-6: Placing the lower base pattern into the flask, making sure to leave room for the sprue. Talcum powder (baby powder) bottle shown sitting on the edge of the flask.

The first pour was completed on September 20th, and the resulting part was broken out a few days later. The part was in good condition and had minimal defects. There was a small hole by the intersection of the flange and the main cavity, which was filled by Pappalardo staff member Steve Haberek, and a few spots that were overfilled due to the pattern slightly collapsing in some sections.

5.3. Finishing the Lower Base

Work for finishing the lower base began in November. The vents on the surface of the casting were removed by Steve Haberek when he filled the hole in the part, meaning that the first step for finishing the part was to remove the rest of the extraneous metal. This included the gates, runner, well, and sprue. Due to the geometry of the part, these components posed some challenges to remove, at one point even resulting in a broken bandsaw blade. Caution must be taken when working with these casting, since the cast iron is very hard, especially along the thinner edge sections due to cooling effects.

Figure 5-7: Core print flash removed from the casting; the more reflective areas being visible indicators of hardened sections due to rapid cooling during casting.

Once the extraneous metal was removed, the part had to be mounted on a mill bed to face the upper surface, which is the surface that connects the lower and upper base parts. In order to face this part, two 123 blocks were placed underneath each corner of the part, and the part was clamped down to the machine bed. The part was mounted such that the upper surface of the lower base and the engine mounting holes could all be faced in the same orientation, taking care to keep the part in the same clamped position until all operations could be completed.

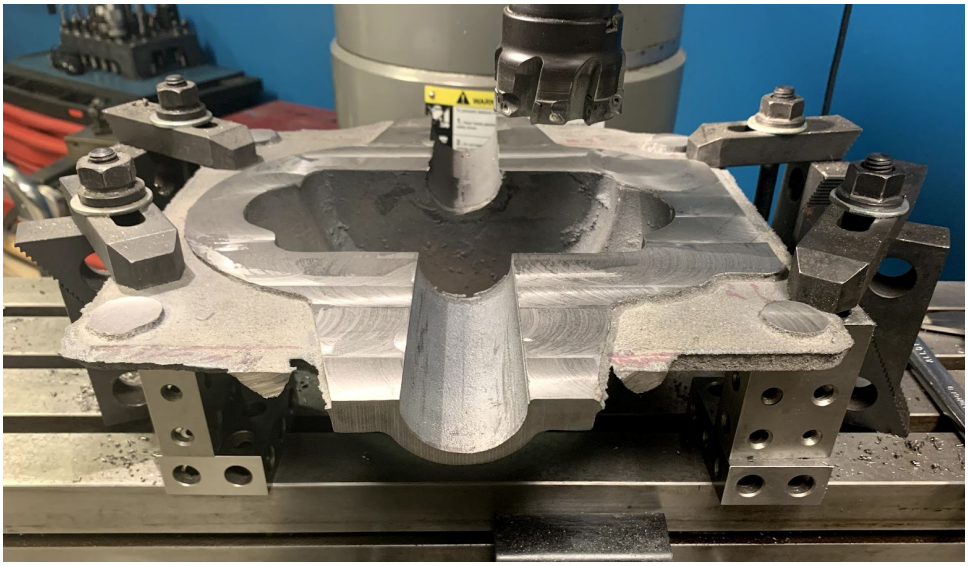

Figure 5-8: Lower base mounted to the bed of a 2-axis mill, supported and clamped on each corner by two 123 blocks; partially faced.

After facing the part, the mounting holes had to be drilled. There are nine 0.5” threaded holes on the mounting surface of the lower base, as well as clearance holes for a 0.5” bolt in each corner of the lower base, which are used to mount the engine to the boat.

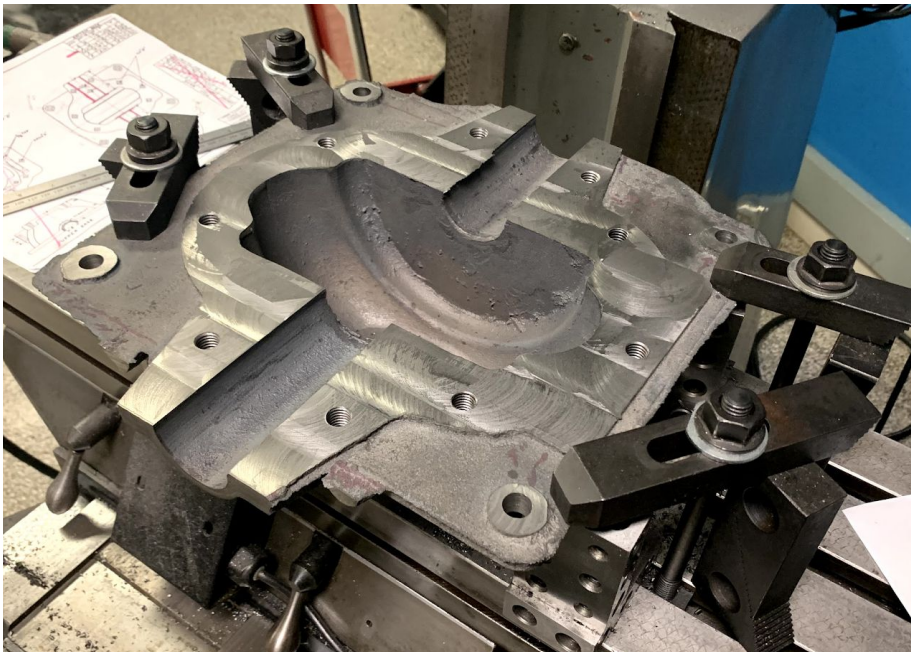

Figure 5-9: Lower base mounted to the bed of a 2-axis mill; completely faced and with holes drilled.

Once the holes were drilled, the last critical step was to cut the bearing surfaces for the crankshaft to the correct length. After this all that remained was to clean up the edges of the casting, for cosmetic and safety purposes, since the rough cast edge is aesthetically unappealing and is a danger to hands and fingers. With the completion of this part, the project was one step closer to a complete engine.

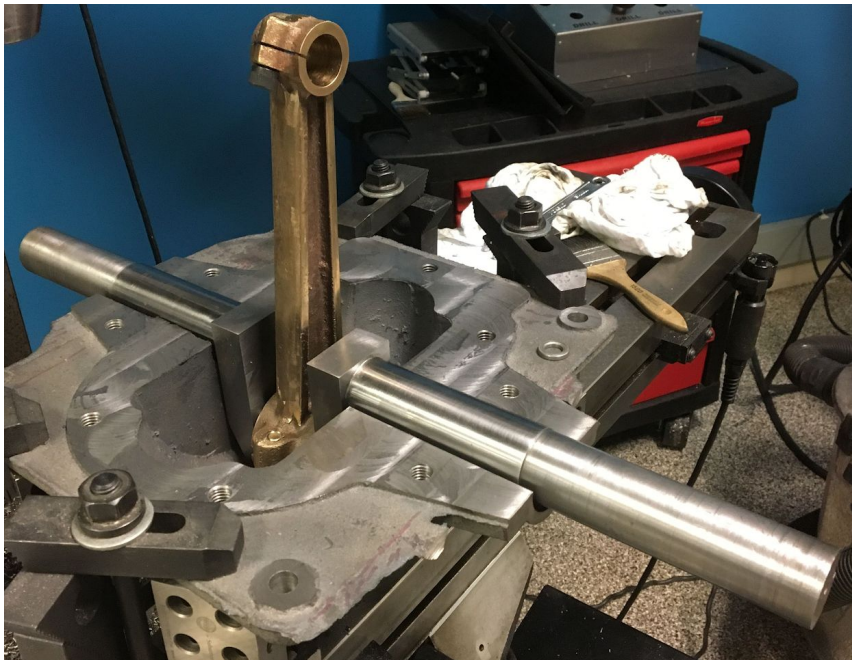

Figure 5-10: The lower base with the crankshaft and connecting rod (crankshaft made by Josh Born and Jarrod Smith Spring 2016; connecting rod made by Sarah Tress Spring 2019), showing the eventual assembly.

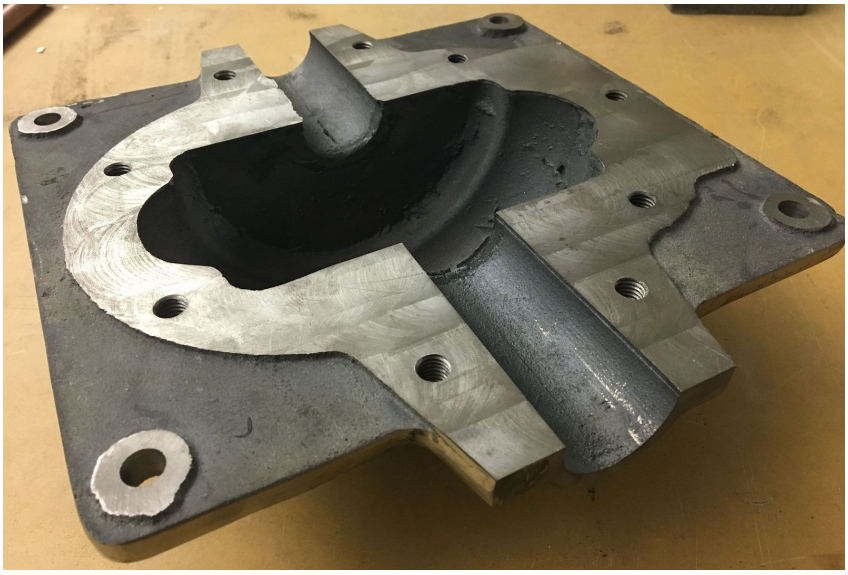

Figure 5-11: Completely finished lower base.

6. The Manifold

The manifold is the component of the engine that acts as the interface between the cylinder and the carburetor-exhaust. In the Atlantic engine, it is mounted directly to the side of the cylinder. The manifold includes three passages: one to allow for the air-fuel mixture to flow from the carburetor to the cylinder, one to allow exhaust to flow out of the combustion chamber, and one acting as a water-pocket to allow water to flow from the cylinder's water-jacket into the manifold for cooling. In order to create these three chambers, the manifold requires a fairly extensive core, and the resulting wall thicknesses are quite thin in comparison to some of the other cast parts in this engine.

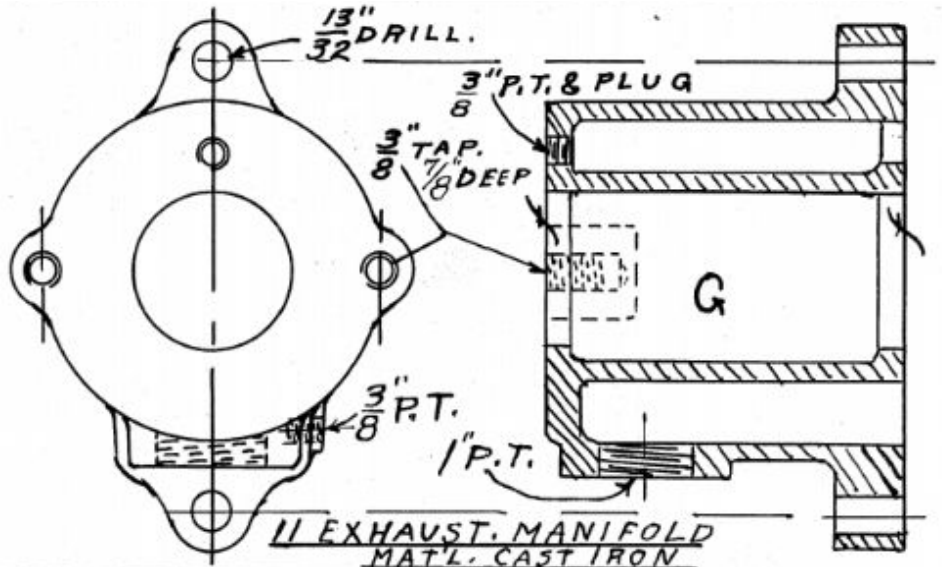

Figure 6-1: Lunenburg Atlantic engine manifold drawing [3].

6.1. Previous Attempts

The first student to work on the manifold was Gordon Mosely P. Andrews, in the spring of 2016. Like Joba-Woodruff, Andrews developed CAD for the part, pattern, and core boxes. Right from the start the manifold posed a challenge because the dimensions of the internal cavities are not very well defined by the drawings. Andrews and the rest of the team interpreted the drawings and made decisions about what they believed the features to be, and Andrews was able to complete a model of the manifold. From there, he developed CAD for the pattern and core box. All components were CNC milled out of high-density polyurethane foam. The pattern functioned perfectly, but the core box was a greater challenge.

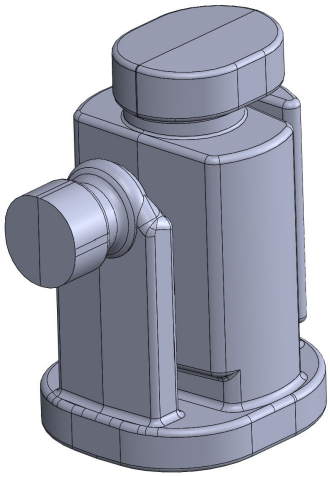

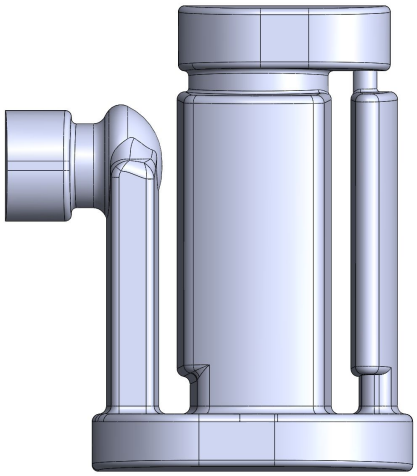

Figures 6-2 and 6-3: Two different views of a CAD model of the manifold core.

Given the core, there are a few weak spots that are quickly identifiable due to the thickness of the material. The first corebox that Andrews created was designed to allow the core to be made in two complete halves, then glued together into one piece.

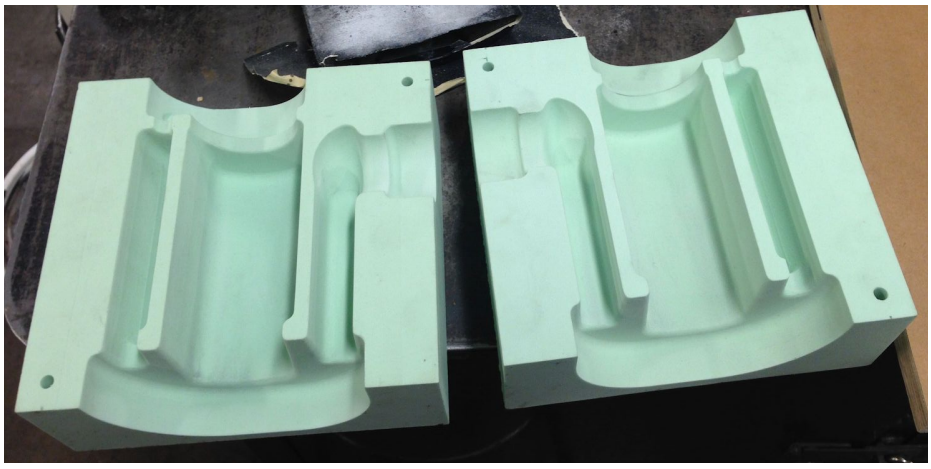

Figure 6-4: Manifold core box, both halves, machined by Gordon Mosely P. Andrews; Spring 2016.

Each half of the core would be made, the two halves would be glued together while still in the core boxes, and the entire core would be removed from the corebox once it had cured. However, upon attempting to remove the core from the core box it was clear that the shear forces along the faces of the core were too significant to remove the core in one piece, and the result was a broken core. Attempts were made to glue the parts together, but it was decided that the resulting core would have lost too much dimensional accuracy.

Figure 6-5: Broken core, created in one piece using the first iteration of the core box, but broken during removal, leaving rough interfaces between components.

From here, Andrews modified the core print to allow for easier removal and reassembly of the core. He added metal shims between the different sections of the core, so that when the core print was packed there would be three discrete parts as a result. The three parts all had clean edges, making it easier to glue them together and maintain the designed geometry.

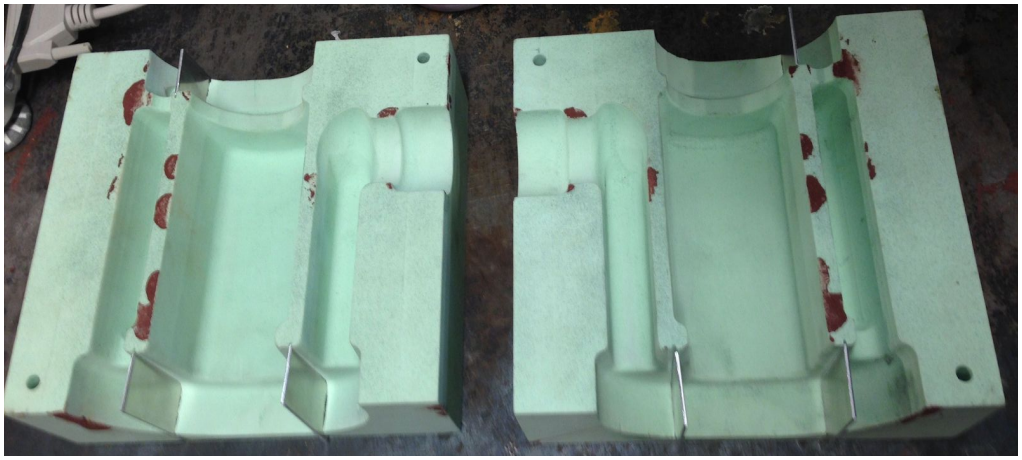

Figure 6-6: Modified manifold core box, adding metal shims to separate the different sections of the core; fabricated by Gordon Mosely P. Andrews; Spring 2016.

With the pattern completed and the new core box functional, Andrews was able to begin casting. Before the end of the academic year, he was able to pour the manifold. The first pour had significant defects - there was a sizable gap between the core prints and the core - and as a result the vent in the exhaust duct section of the core was filled with iron, meaning that there was not enough iron to complete the critical walls.


Figures 6-7 and 6-8: Two views of the first attempt to cast the manifold, showing the fill defect; fabricated by Gordon Mosely P. Andrews; Spring 2016.

The second attempt did not have as severe issues, and externally was completely filled and had much less flash than the first attempt, but the internal chambers had several regions of incomplete fill. This was likely due to trapped gases, and resulted in diminished quality of internal features.


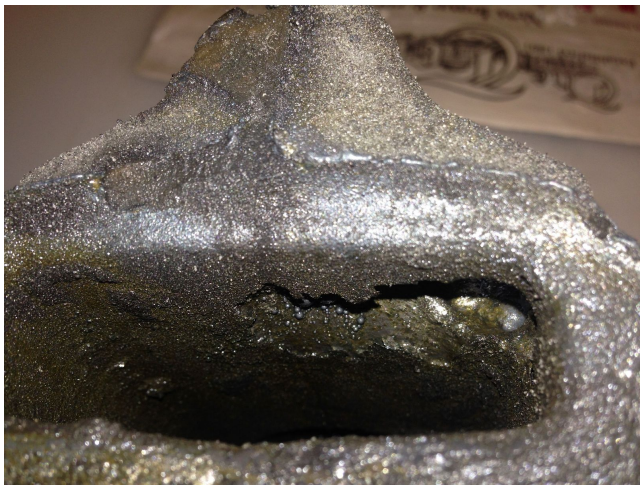

Figures 6-9 and 6-10: Left image showing the decreased flash on the second casting attempt; right image showing the internal cavity defects; fabricated by Gordon Mosely P. Andrews; Spring 2016.

Another attempt resulted in large voids within the thin walls of the part, making it much more fragile than intended. The voids were present in the portion of the part that was located in the cope, the upper section of the flask, indicating that the fill orientation and venting could have been an issue.


Figures 6-11 and 6-12: Two views of a manifold casting attempt, cut in half to show the void found within the thin wall; fabricated by Gordon Mosely P. Andrews, Spring 2016.

While his attempts were unsuccessful, he was able to set a very strong foundation for continued work and provide learning examples for ways in which pours can fail, which is critical to developing a general understanding of iron casting.

In the spring of 2019, Matt Quejada took on the task of recreating the manifold. He developed a new pattern that involved much larger core prints. The increased area would ideally allow the core to sit fully within the flask and be held securely during the pour, preventing the severe flash issue Andrews saw in his first pour attempt. Along with modifying the core prints in the pattern, Quejada also modified the core box. To decrease the stress on the walls and provide more sand empathy, Quejada split the core print into six different sections. This would allow each portion of the core to be removed individually, and hopefully would decrease the likelihood of the core breaking during removal. Due to time constraints he was not able to iterate on the core box set-up as much as he would have liked, and as a result the core still posed a challenge.

Once Quejada had finished making modifications to the pattern and the core box and machined the new patterns, he was able to begin casting. Since the patterns all had to be remachined, Quejada was only able to pour the part once. When machining the patterns, he realized that the scaling had been off, meaning that the part would be larger than intended. Despite this error, a pour was attempted. However, for a variety of reasons the resulting part was a failure.


Figures 6-13 and 6-14: Left image showing manifold casting attempt, showing short shot; right image showing manifold casting attempt right after being broken out, showing the section of the core print that filled unintentionally; fabricated by Matt Quejada, Spring 2019.

This failure was likely due to a few different issues. One, because the core prints were so incredibly large, the runner distance was quite long. This extra distance was not accounted for when pouring, so the part ended up being a short shot. Additionally, because it had to travel such a far distance, the iron cooled down considerably by the time it hit the pattern, making the already challenging flow path even more difficult to fill. After breaking out the part it was discovered that the iron had filled an air pocket in the core print that the team had not been aware of, meaning that the material was redirected and unable to fill the walls of the manifold. From all of these attempts, it is clear that filling this part properly is a real challenge, and that successfully completing the part may require taking it from a different angle.

6.2. Pattern and Mold Fabrication

When making an attempt to recreate the manifold in the spring of 2020, it was very clear that there was an incredible wealth of work existing for this part. However, this also meant a great quantity of different patterns and core boxes. After examining the existing parts, patterns, and core boxes, the decision was made to use the patterns created by Andrews in the spring of 2016, because the smaller core print would decrease the amount of resin bonded sand necessary for the core and would allow for a slightly smaller flask to be used, meaning less green sand, less work packing the flask, and a shorter runner length. The core box was redesigned to further increase the sand empathy and fit the core print. The new core box was created in seven parts, with parting lines placed to allow for the most sand empathy possible.

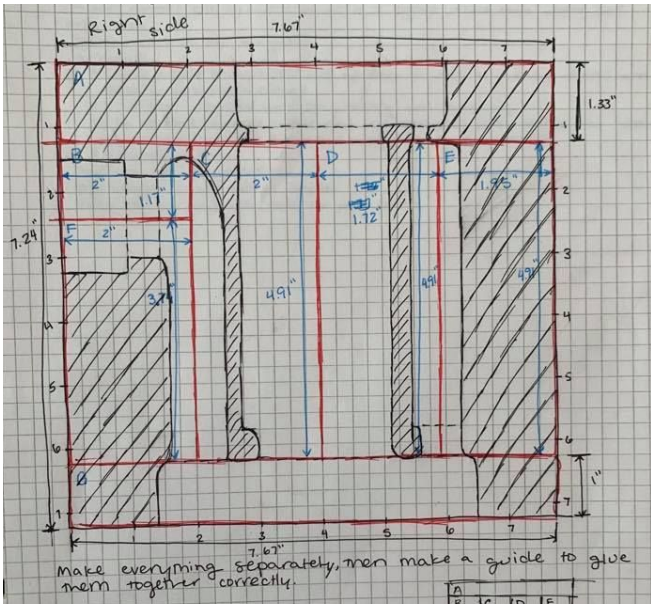

Figure 6-15: Notebook sketch planning out the layout of the redesigned core box, showing parting lines and dimensions.

Following suit, the new core box was created using the high-density polyurethane on the CNC mill. To make sure that each section of the core box was properly aligned, the parts were machined as though the core box was a single piece of foam. To start, the foam was cut to match the dimensions of each part, and they were clamped together to create a single block. This assembly was then clamped into the vice of a 3-axis CNC mill, with clearance to make sure all of the open edges of the core box would be machined without hitting the edge of the vice and with consideration of the y-limit of the machine.

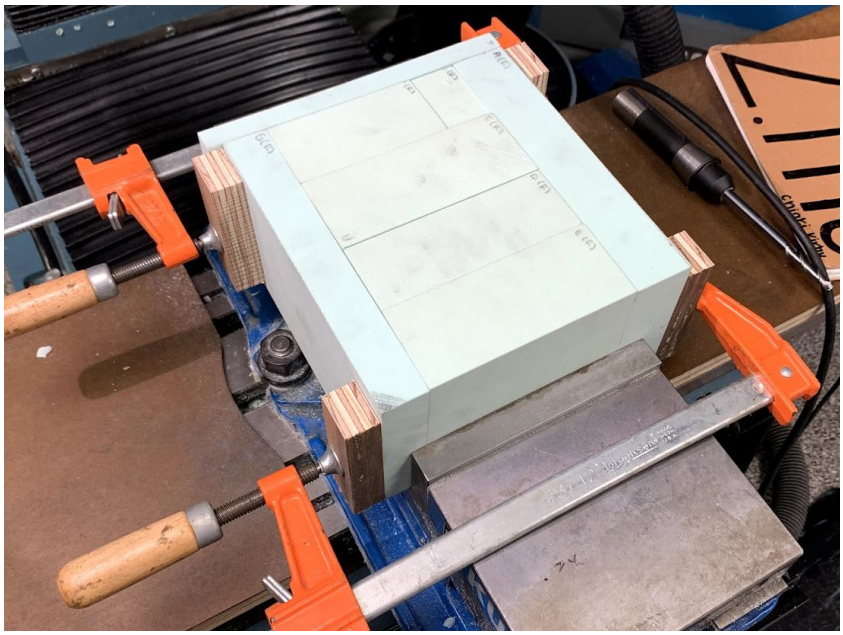

Figure 6-16: Redesigned core box set-up, with seven part block clamped together and clamped into vise.

Once set up, the core box was milled as though it were one piece of foam. Since the manifold is not an incredibly large part, the core print job was quite quick once the set-up was complete.

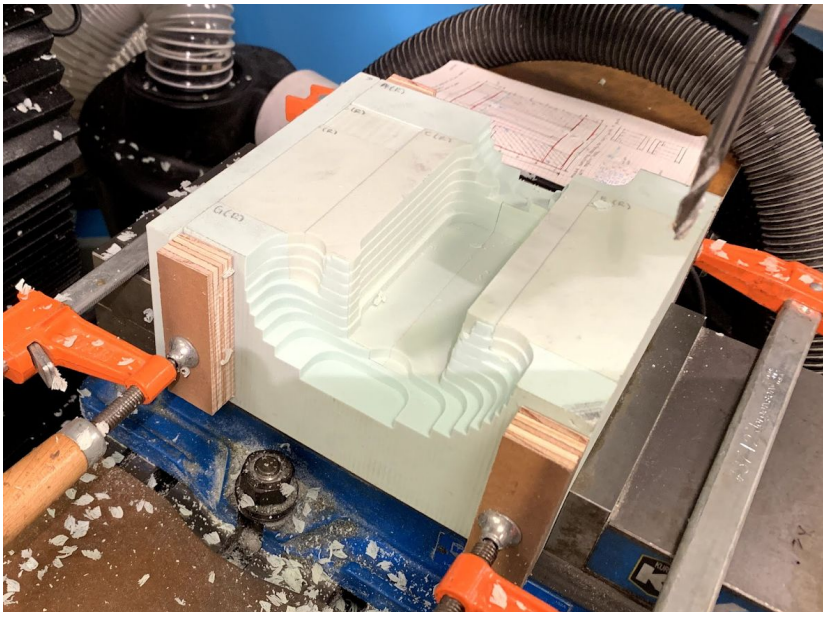

Figure 6-17: Redesigned core box part way through machining.

Due to the way the components had been divided and the human error when cutting the initial foam segments, there were some sections of very thin foam that were ripped off in the machining process. This created very minor defects that were predicted to have minimal impact on the overall core.

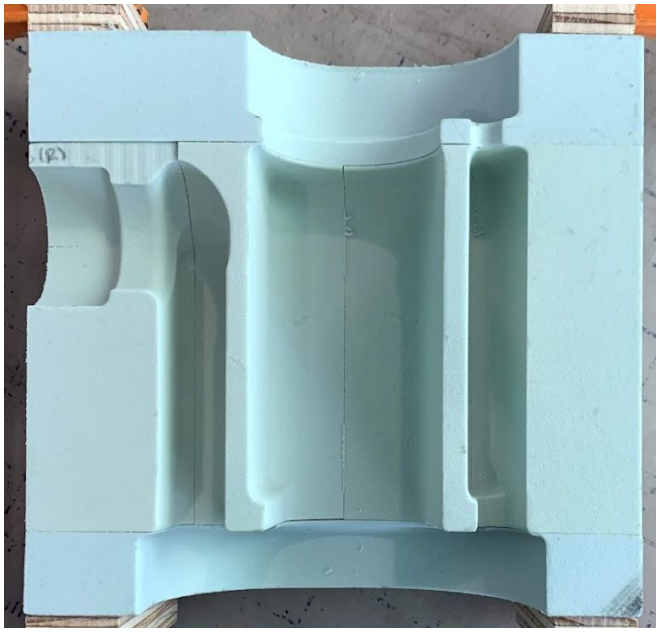

Figure 6-18: Completed core box, showing how the seven components fit together to create the core.

With the new core box, the three internal chambers are created with a set of five parts, to create each chamber individually. The upper and lower core prints are then created on their own, and the entire core is assembled and glued together. The goal was to make sure that each segment of the core print could be made with minimal defects, while also making it easy to remove each component, easy to use the core box, and easy to assemble the full core once each component had been made. Right before MIT closed the campus due to the COVID-19 pandemic, the new core box was used to create a core. The core was not completely assembled, as it was curing during the final days before campus closure, but the core box released easily and the components came out with few defects; ready to be glued together to create the entire core.

Figure 6-19: Half of the manifold core, created out of resin bonded sand using the redesigned core box.

6.3. Considering the Pour Orientation

When creating a casting, parts are split along a plane called the parting plane, which is selected to avoid undercuts and make creation of any cores or sliding sections simple. For this manifold, the parting plane had been selected to split the part into two mirrored parts, to allow for ease of pattern and core creation and usage. Using the traditional two part flask system, half of the pattern would be placed in each part of the flask, so one half in the cope and one half in the drag. The part would then be cast lying on its side, in the same orientation that it is mounted to the side of the cylinder. From the first pour of the manifold in the spring of 2016 to the final pour in the spring of 2019, the manifold was consistently poured in this orientation. A casting created in the spring of 2016 had serious void issues, as discussed in section 6.1: Previous Attempts. The void issues were located in the section of the part that was in the cope, leading to the thought that changing the pour orientation from horizontal to vertical could alleviate this issue.

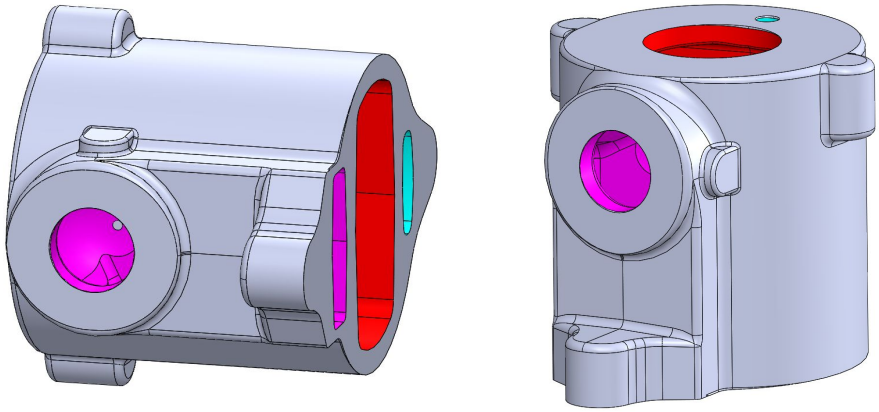

Figures 6-20 and 6-21: Left image showing the manifold in the horizontal orientation; right image showing the manifold in the vertical orientation.

The idea was that by shifting the pour orientation, the thin wall segments would be filled evenly from bottom to top, allowing for consistent filling throughout the entire part. Since the wall segments are so thin, creating symmetry in the way they are filled would help ensure they fill completely and equally. By filling from the bottom to the top the gas would be pushed out of vents in the top of the flask and the flask could be completely filled with iron. Additionally, when in the vertical orientation the iron would be able to fill evenly around the core, building solid walls throughout the inside of the manifold.

In order to accomplish this, a three part flask would have to be made. The flask would consist of a drag and a two part cope, to allow the pattern to be almost entirely placed in the cope without having any issues with undercuts.

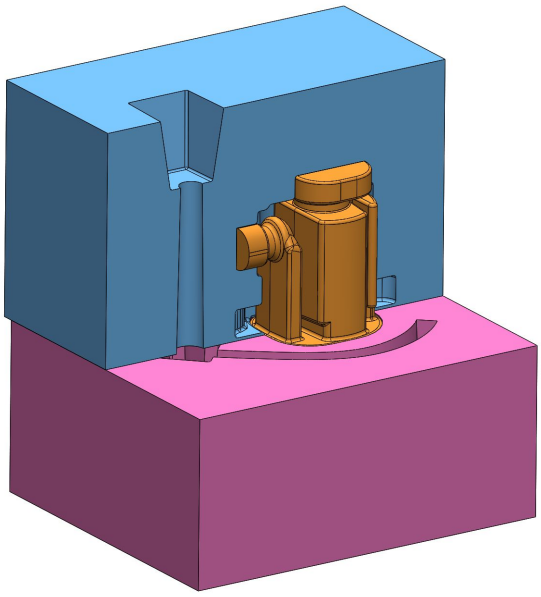

Figure 6-22: CAD of three part flask, with half of the cope hidden to show the internal features (including the core, gates, runner, sprue, well, and pour basin)

The flask was designed with the manifold split along the same parting plane as it had been in previous attempts, but with the lower core print separated from the main body. This was so the lower core print could be in the drag while the rest of the pattern was in the cope, so that the gates could be cut into the bottom surface of the cope and run directly into the casting. The sprue and pour basin were also split along the parting plane, so that they could be packed into the cope along with the pattern.

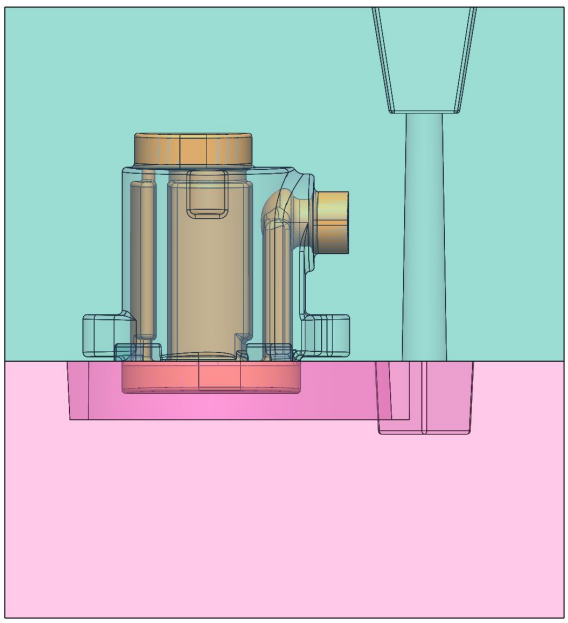

Figure 6-23: Side view of the flask, with transparency adjusted to show the core fitting into the core prints.

The drag was designed to be packed around the runner, lower core print, and well. By machining patterns for these components rather than carving them by hand, the ideal alignments and cross sections could be calculated and applied, to maximize the odds of a successful pour as shown when Tom Frejowski machined patterns for gating the piston in the spring of 2019.

The flask was built out of wood, taking the spacing of the internal components into account. When creating the cope, the planks had to be assembled such that the ends could be removed to open up the pour basin and sprue on either end. This meant that the end planks had to cap the ends of the flask. The process to fill the flask involves first filling the cope, then removing some of the sides, then filling the drag. Specifically:

1. Pack one half of the cope (not critical which side is filled first) using the manifold, sprue, pour basin, and gate patterns.
2. Flip the packed half, and pin the other halves of the manifold, sprue, and pour basin patterns to the packed halves.
3. Pack the rest of the cope.
4. Clamp the two parts together.
5. Attach plywood to the open sides of the cope.
6. Remove the planks of wood on the top and bottom of the cope component of the flask.


Figures 6-24 and 6-25: Left image showing a top view of the cope, with one of the top planks removed; right image showing the cope with one of the top planks removed, with a clear view of the interlocking and clamping mechanisms and the plywood side panel.

7. Flip the cope, and pin the runner, well, and lower core print patterns to the patterns in the cope.
8. Pack the drag.

Figure 6-26: The drag component of the three-part flask.

9. Clamp the drag and cope together.
10. Flip the entire assembly into the correct orientation (with the pour basin on the top plane).

Figures 6-27 and 6-28: Two different views of the fully assembled three-part flask, showing the interlocking locating features, clamping surfaces, and the additional plywood panels.

Unfortunately the MIT campus closure occurred before this flask could be used to create any castings, but further developed CAD models and simulations indicate that this flask should be functional and result in a complete casting.

6.4. Designing the Filling System

In the past, most of the castings completed as a part of the Pappalardo apprenticeship have had many of the pattern features carved into them by hand. This includes the well, the runner, the gates, and the pour basin. As mentioned in the previous section, when creating the piston Tom Frejowski applied equations for gating and risering to create high-density polyurethane foam patterns for the features included in his flask, in order to make sure the part would fill properly. This can be done using an incredibly detailed text, “Ductile Iron: The Essentials of Gating and Risering System Design” [6].

In a casting, the choke is the section of the runner that determines the mold filling time. Gate-runner systems involve choking each casting individually, while sprue-runner systems use a common choke for several castings. Since the manifold is one casting gated in multiple places, a combination gate-runner and sprue-runner system was designed. There are a number of variables that need to be selected in order to determine the cross sectional areas of the choke, runner, and gates. These depend on the geometry of the casting and flask, such as the volume of the casting and the effective ferrostatic head in the sprue.

The first calculation determines the choke cross sectional area. The equation used has different forms for being entirely in the cope, entirely in the drag, and in both the cope and the drag. The vertical

orientation of the manifold casting is entirely in the cope, while the horizontal orientation is in both the cope and the drag.

- When casting located entirely in cope,

$$A_c = \frac{1.5\,(b)\,V_C}{f_r.t.\sqrt{2g}\;\left[\sqrt{H^3} - \sqrt{(H-b)^3}\right]}$$

- When casting located in cope and drag,

$$A_c = \frac{1}{f_r.t.\sqrt{2g}}\left[\frac{V_D}{\sqrt{H}} + 1.5\,(b)\,\frac{V_c}{\sqrt{H^3} - \sqrt{(H-b)^3}}\right]$$

Figure 6-29: Equations for determining the cross-sectional area of the choke [6].

The variables that the choke cross-sectional area depends on are the friction loss factor (f_r), the pouring time (t), the total poured volume/choke (V), the effective ferrostatic head in the sprue (H), and the height of the casting in the cope (b). Aside from the friction loss factor and pouring time, these are all directly determined from the casting and flask. The friction loss factor is based on the weight of the casting, with generalizations for thin "plates" and heavy "cubes", as well as a more specific curve.

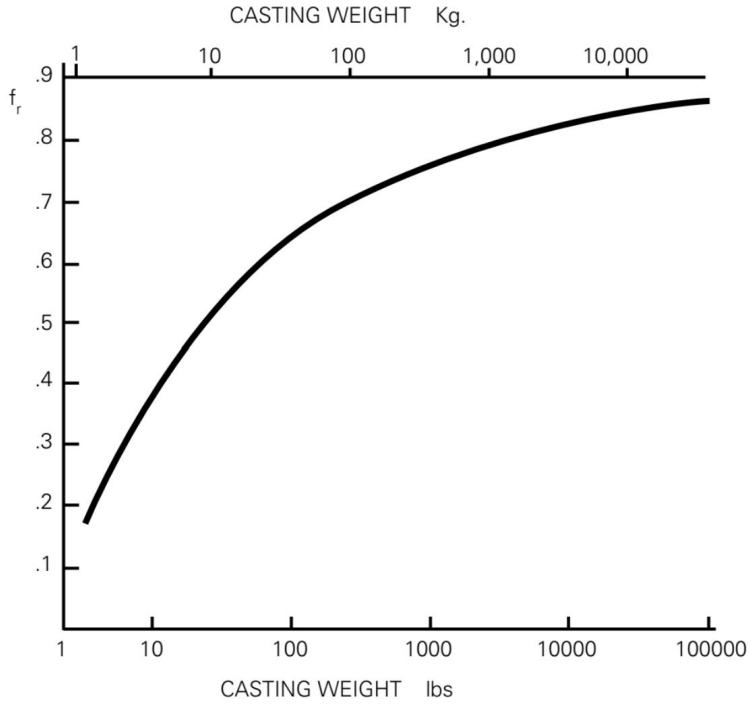

Figure 6-30: Curve used to determine the friction loss factor based on casting weight [6].

Similarly, the pouring time is determined by the weight of the casting, including the risers, per choke. There is a curve for determining the pouring time, and additionally there is a general equation based on the weight of the casting and risers.

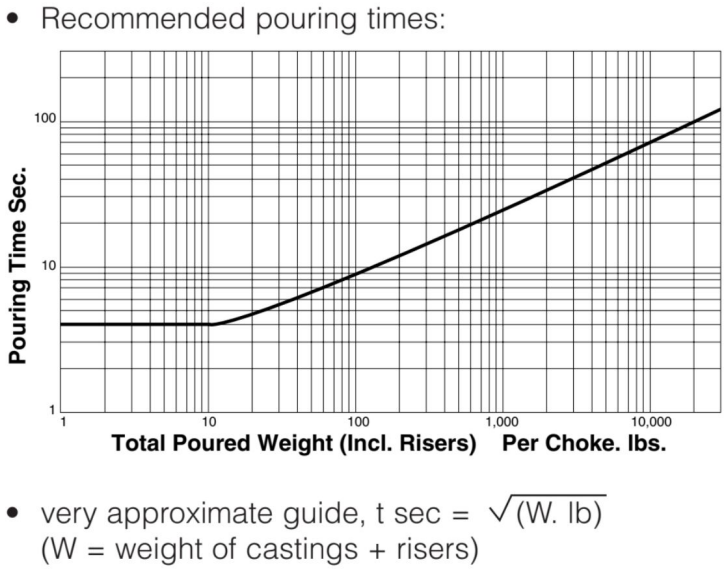

Figure 6-31: Curve used to determine the pouring time based on casting and riser weight; general equation relating pouring time and weight of casting and riser weight [6].

Once the choke cross-sectional area has been determined, it can be used to calculate the gate, runner, and sprue cross-sectional areas. The gate cross-sectional area is determined by dividing the choke cross-sectional area by the number of gates. This is then used to determine the dimensions of the gate, described as 4a by a. In the horizontal orientation of the manifold, there are two gates. In the vertical orientation, there are four gates. The runner cross-sectional area (A_R) is three times the choke cross-sectional area. This is then used to determine the dimensions of the runner, described as 2a by a. The sprue cross-sectional area (A_S) is based on the effective ferrostatic head in the sprue (H) and the distance from the top of the flask to the smallest cross-section of the sprue (h). The sprue is generally tapered, so this distance changes based on the direction of taper. In the manifold castings, a downward tapered sprue was used, meaning that h was the depth of the pour basin.

$$A_s = A_c \sqrt{\frac{H}{h}} (\text{minimum})$$

Figure 6-32: Equation to determine the minimum sprue cross-sectional area [6].

The last features to be determined are the pour basin and the sprue well. The pour basin width (W) can be selected based on the diameter of the sprue. The guidelines are not incredibly specific, only that the width of the pour basin should be greater than the diameter of the sprue. The basin should then be a rectangle of W by W by 2W. The sprue well is also determined by the diameter of the sprue (D). The well is essentially a tapered cube, with side length 2D.

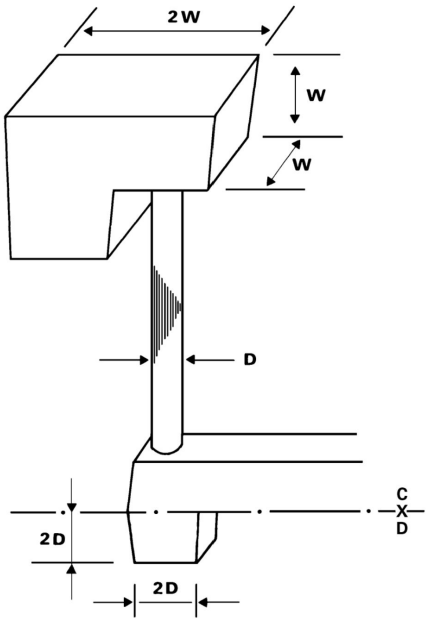

Figure 6-33: Image depicting dimensions of the pour basin and the sprue well [6].

Additionally, the text describes the best orientation of these different components, and ways that they should interface. Features such as the overlap of the runner and gates, the geometry of the runner, and the taper of the runner.

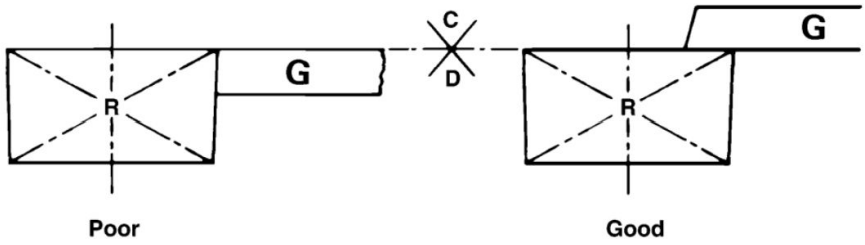

Figure 6-34: An example of best practices for gate and runner interfacing in sprue-runner systems [6].

6.5. Simulation Results

At the start of the 2019-2020 academic year, the plan for this project was to finish the remaining parts. After completing the lower base part in the fall, the first part in the works during the spring was the manifold. The initial plan, as mentioned above, was to pour the manifold vertically using a three part flask, to test if changing the pour orientation would minimize the voids caused by gases inside the flask. However, the sudden closure of the campus prevented any non-essential research, bringing the fabrication component of this project to a halt. To accomodate for the switch to entirely virtual coursework, this thesis project became focused on specific analysis of the manifold. Using virtual casting software, the manifold molds were created in CAD to create simulations of the pours. While not the same as physically doing the pour, it allows for easier testing of a variety of orientations and component layouts, and gives a much more detailed view of what is predicted to occur than the information one can gather from a

physical part. That being said, the results of the simulations are somewhat idealized, given that the mold, the core, and the physical pour will not be as perfect as the simulation likely predicts.

One of the most significant idealizations is the degree that the mold is filled. In the simulation, the percent fill is selected. Convention is to set the fill at 98%, since that is at least more realistic than 100% fill, but in reality it is hard to confirm if enough material has been poured, and a short shot can be the cause of failure, especially when the molten metal is slow to fill some of the smaller cavities in the mold. Another issue is that the molds and cores are exactly as designed. When packing the mold, it is entirely possible that there are small defects or that the core does not fit perfectly, meaning that the chambers are not exactly as designed. This is likely a small detail that does not contribute in a very significant way, but it is still an idealization that the model makes.

The simulations give results related to heat, flow, and other selected parameters. Once the calculations have been run, the software is capable of showing the flow pattern of the molten metal into the mold, showing how the flow of metal can be hindered by certain features, the likelihood of certain cavities to fill, and any shrinkage or other defects that may occur. There are a variety of variables that can be examined, such as the temperature of the metal through filling and solidification, the time to fill, and the solidification time.

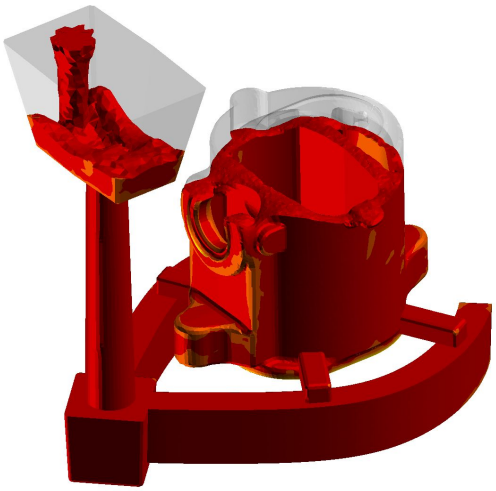

Figure 6-35: Example of the simulation, showing the temperature of the metal during filling using a color scale, with the red indicating the starting temperature of 1250 °C.

For the purposes of this project, the fill of the part is most critical, so the porosity defects and voids are the results that are of greatest concern. Simulations were run to test a variety of orientations and configurations, and the resulting porosity and void defects were compared to determine the best flask set-up of the tested set-ups. The manifold was simulated in the horizontal orientation, with gate runners and gates feeding the metal from the bottom flanges. The manifold was also simulated in two vertical orientations, the first a simple gated system and the second a modification that increased the size of the gates and added a riser for improved filling. All three of these simulations were run with an initial pour temperature of 1250 °C, and the second vertical orientation was additionally run at 1300 °C and 1350 °C to see how pour temperature affects the final part.

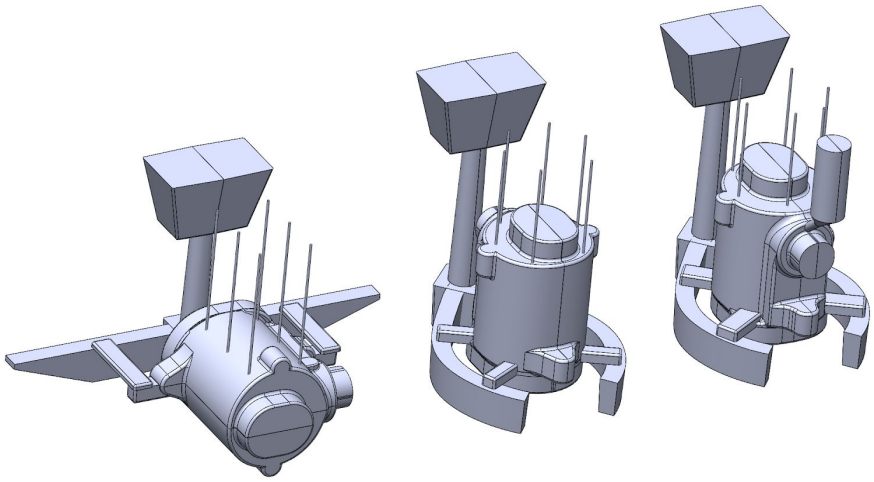

Figure 6-36: CAD models of the three manifold set-ups, following the listed order above.

The different manifold set-ups were chosen to illustrate the differences between the horizontal and vertical results, and the second vertical orientation was tested to see if other changes could improve the quality further.

The simulation results for the horizontal casting show a significant spread of porosity defects, as shown in the yellow highlighted sections of the simulation image below.

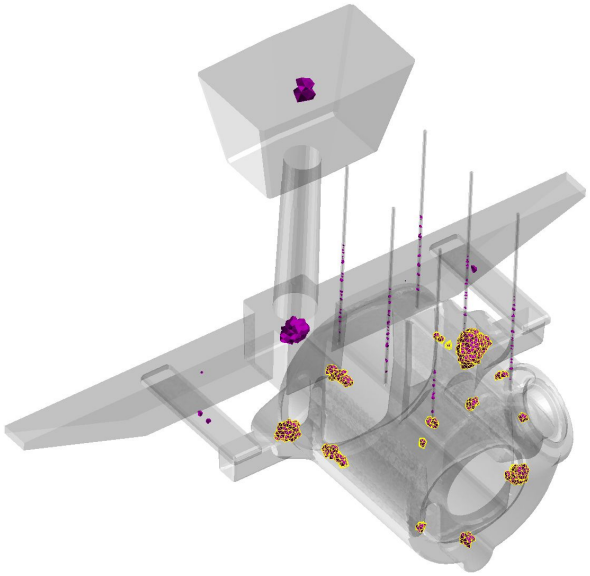

Figure 6-37: Results for the horizontal orientation, showing porosity defects; initial pour temperature of 1250 °C.

The porosity volume is 4.019 cm^3, or 0.245 in^3, which is not an incredible amount compared to the total volume of 48.19 in^3 but is spread enough throughout the part that it may cause issues with the functionality of the part under high pressure. The results also show that there are no voids found in the part. Overall the quality of the part is decent, showing that the simulation can idealize the pour since none of the past attempts at creating this part in this orientation have been successful.

The simulation results for the first vertical casting show interesting defects. Similarly to the horizontal pour, there are porosity defects to be found in the part.

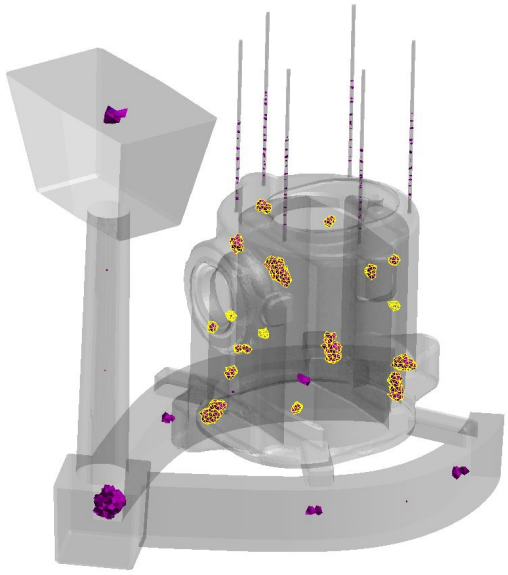

Figure 6-38: Results for the first vertical orientation, showing porosity defects; initial pour temperature of 1250 °C.

The porosity volume is 1.265 cm^3, or 0.077 in^3, which is a noticeable decrease compared to the horizontal orientation. However, while there are no voids in the horizontal orientation, there is a void in the vertical orientation right above the air-fuel intake duct.

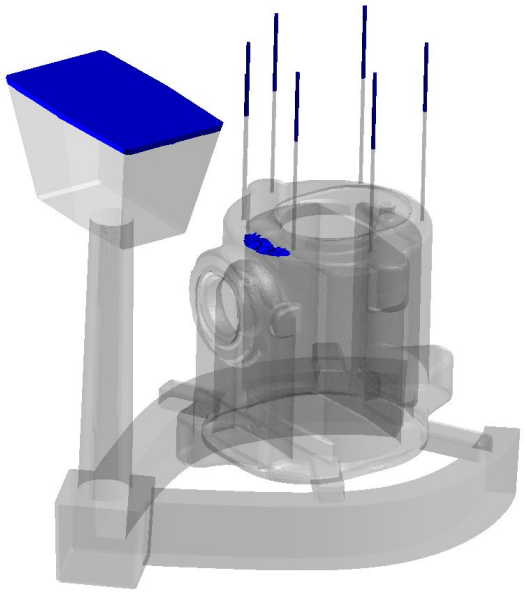

Figure 6-39: Results for the first vertical orientation, showing voids; initial pour temperature of 1250 °C.

While it is unclear if the porosity defects would have a significant impact on the functionality of the part, it can be assumed that a void of this size would be a concern and would likely mean the part needed to be remade. This goes against the expectation that the vertical orientation would result in a higher quality part, but again could be due to idealizations made by the simulation that would not actually occur in a real-life pour. The void indicates that it might be necessary to include a riser in order to make sure that the part fills completely. Generally, the senior apprenticeship castings have not included risers for cast iron parts because cast iron does not undergo solidification shrinkage, meaning that having a surplus or "bank" of metal to maintain the fill is not critical because the metal does not shrink as it goes from liquid to solid. In this case, since the void is near the top of the part it may be helpful to include a riser to make sure the gas is released and the part fills completely.

The final simulations were of a modification of the vertical orientation, as discussed at the start of this section. The gates into the part were increased, with the width changing from 0.7" to 1.05". Additionally, there is a riser attached by the air-fuel intake duct, to prevent the void from occurring. This part was simulated at three temperatures to evaluate how the defects may change based on initial pour temperature. The first attempt was run at 1250 °C. As expected based on the prior orientation results, there are porosity defects throughout the part.

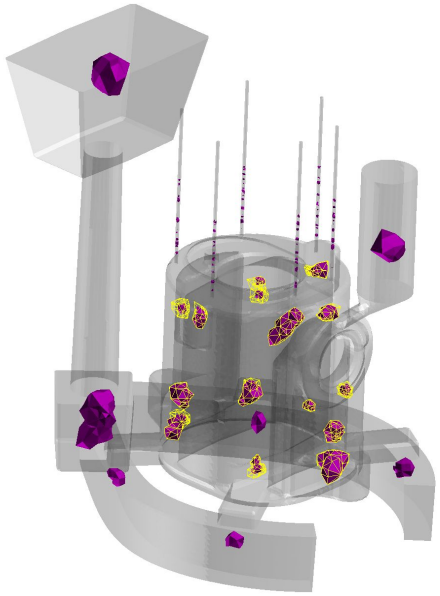

Figure 6-40: Results for the second vertical orientation (including riser), showing porosity defects, initial pour temperature of 1250 °C.

The porosity volume is 1.289 cm^3, or 0.079 in^3, which is a minor increase from the original vertical orientation results. This is a very minor difference, and does not give an indicator of which set-up is better. However, with the larger gates and riser included, the part does not have any voids.

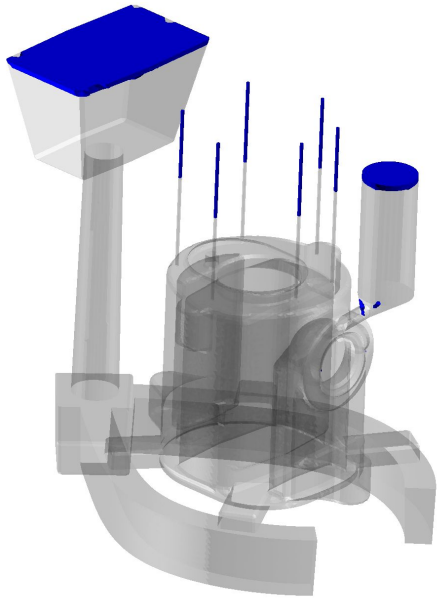

Figure 6-41: Results for the second vertical orientation (including riser), showing voids; initial pour temperature of 1250 °C

The second attempt was run at 1300 °C. As with all of the former tests, there are porosity defects throughout the part.

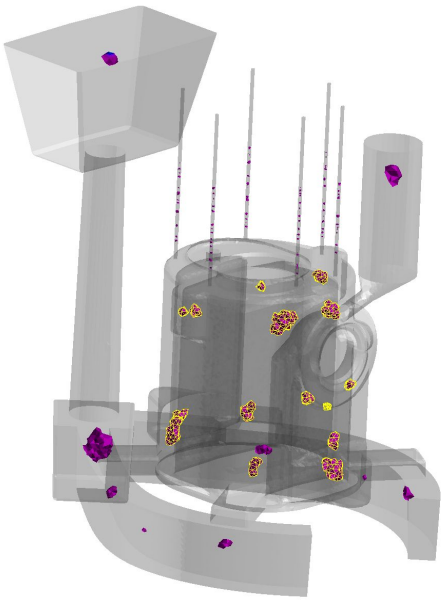

Figure 6-42: Results for the second vertical orientation (including riser), showing porosity defects, initial pour temperature of 1300 °C.

The porosity volume is 1.100 cm^3, or 0.067 in^3. This is a fairly noticeable difference from the same part run at 1250 °C. Similarly, there are no voids in this part as well.

The third and final attempt was run at 1350 °C. Once again, there are porosity defects to be found throughout the part.

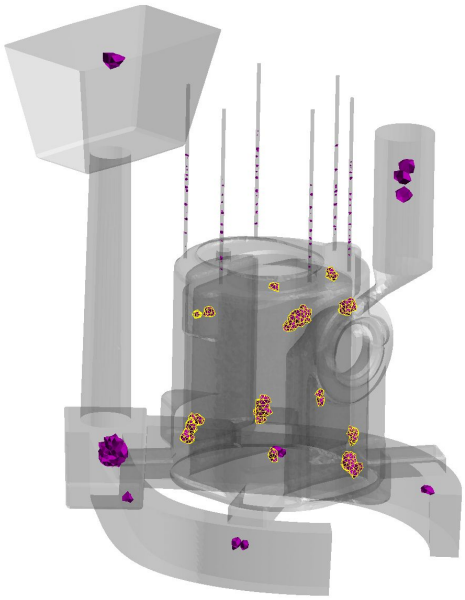

Figure 6-43: Results for the second vertical orientation (including riser), showing porosity defects, initial pour temperature of 1350 °C.

The porosity volume is 0.938 cm^3, or 0.057 in^3. This is a further decrease in porosity volume, indicating that having a higher initial pour temperature is beneficial for minimizing the porosity volume. Similarly, there are no voids in this part as well.

The second vertical orientation, cast with an initial pour temperature of 1350 °C, has the smallest porosity volume as well as no voids, showing that it has the highest quality final part out of the set-ups tested. In order to confirm that this set-up leads to successful parts, additional simulations should also be run to test modifications of other parameters, such as adding a riser to the horizontal orientation or testing the other set-ups with different initial pour temperatures. The part should also be physically cast to allow comparison between the tangible results of this set-up and the past horizontal set-up attempts.

7. Next Steps

7.1. The Manifold

The next major step for this project, once fabrication is possible again, is to fabricate the manifold. Using the understanding gathered about the pour orientation and component layout in this thesis, a pour should be attempted. The three-part flask is near complete, with only a few clamping details to add. The core box is complete and based on the test part it should be fully functional. The most significant modification required is to recreate the pattern. While creating more in depth CAD models of the three-part flask, it became clear that the lower core print needed to be a separate component, meaning that the pattern has to be remachined to take this into account. Additionally, if interested, whoever

continues the project will have the capacity to machine patterns for the sprue, runner, gates, pour basin, and well in order to provide more intentional design to the casting. A critical detail to keep in mind is that while the simulations may give very good indications of the eventual quality of the castings, the physical castings will help expand understanding of the processes as well, and each pour should be done with the understanding that it might not succeed, and there may be an even better way to create the part. Changes should be made not solely based on the simulation data, but also based on the real-life lessons learned from casting.

7.2. Additional Remaining Parts and Finishing Steps

In addition to the manifold, there are two other parts left to be made. The upper base has seen decent success, and the existing patterns are a great starting point for fabricating the part. With analysis of the existing attempts, patterns, and CAD, as well as possible recreation of patterns, the upper base should be a manageable part to recreate. Creating the cylinder poses a much more significant challenge. Attempts have been made to fabricate this part, including a very strong attempt by Shannon McCoy in the spring of 2019, but the massive size of the cylinder combined with the complexity of the cores and water jacket make this part quite difficult. There is a solid foundational body of work on this part, and with guidance, assistance, and perseverance the part can (and will) be made. With this final part, the engine will need to be assembled, including adding babbit to bearing surfaces, and components will need to be tested before the Atlantic engine will be able to run. The long term goal is to bring the completed engine to the Foundry, and this is close to being a reality.

8. References

[1] Lunenburg industrial foundry & engineering: Our history. Accessed May 4, 2020. https://www.lunenburgfoundry.com/company/our-history

[2] Grayson, Stan. “American Marine Engines”. Marblehead, MA: Devereux Books, 2008.

[3] Young, Charles and Young, Daniel, 1929, *Atlantic One-Lunger Engineering Drawings*. Lunenburg Foundry & Engineering Limited, Lunenburg, Nova Scotia.

[4] Powered Parachute Flying Handbook: Chapter 4 - Powerplants. Accessed May 4, 2020. http://avstop.com/ac/power_parachute/chapter4_1.html.

[5] Sherman, D. (12/17/2009) A two-stroke revival, without the blue haze. *New York Times*. Accessed May 4, 2020. https://www.nytimes.com/2009/12/20/automobiles/20STROKE.html

[6] “Ductile Iron: The Essentials of Gating and Risering System Design”. Rio Tinto Iron & Titanium Inc., 2000.